

# Couplings between holographic dark energy and dark matter

Yinzhe Ma,<sup>1,2</sup> Yan Gong,<sup>3,4</sup> and Xuelei Chen<sup>3,1</sup>

<sup>1</sup>*Kavli Institute for Theoretical Physics China,  
Institute of Theoretical Physics, Chinese Academy of Sciences,  
P.O.Box 2735, Beijing 100080, China*

<sup>2</sup>*Institute of Astronomy, University of Cambridge,  
Madingley Road, Cambridge CB3 0HA*

<sup>3</sup>*National Astronomical Observatories,  
Chinese Academy of Sciences, Beijing 100012, China*

<sup>4</sup>*Graduate School of Chinese Academy of Sciences, Beijing 100049, China*

We consider the interaction between dark matter and dark energy in the framework of holographic dark energy, and propose a natural and physically plausible form of interaction, in which the interacting term is proportional to the product of the powers of the dark matter and dark energy densities. We investigate the cosmic evolution in such models. The impact of the coupling on the dark matter and dark energy components may be asymmetric. While the dark energy decouples from the dark matter at late time, just as other components of the cosmic fluid become decoupled as the universe expands, interestingly, the dark matter may actually become coupled to the dark energy at late time. We shall name such a phenomenon as *incoupling*. We use the latest type Ia supernovae data from the SCP team, baryon acoustics oscillation data from SDSS and 2dF surveys, and the position of the first peak of the CMB angular power spectrum to constrain the model. We find that the interaction term which is proportional to the the first power product of the dark energy and dark matter densities gives excellent fit to the current data.

## I. INTRODUCTION

A number of astronomical observations, such as type Ia supernovae (SNIa) [1], the cosmic microwave background (CMB) anisotropy [2], and the large scale structure (LSS) [3], has shown that the expansion of our universe is accelerating. The acceleration of the Universe

strongly indicates the existence of a mysterious exotic matter, named dark energy, which has negative pressure and takes the largest proportion of the total density in the Universe. The ultimate fate of our Universe is to be determined by the dark energy, yet we know little about its properties. Furthermore, while both the dark matter and the dark energy is commonly thought to interact weakly with ordinary matter, it is not immediately clear whether there is some interaction between the two, or if the two are in some way linked.

In this paper we consider the dark matter-dark energy interaction in the framework of the holographic dark energy (HDE) model [4, 5, 6, 7]. The basic ideas of the HDE model is based on the holographic principle [8], which was inspired by the Bekenstein entropy bound of black holes[9]. In this model, the dark energy is related the quantum zero-point energy density  $\rho_\Lambda$ , the total energy of the whole system with size  $L$  should not exceed the mass of a black hole of the same size, thus we have  $L^3\rho_\Lambda \leq LM_{\text{pl}}^2$ . The largest infrared cut-off  $L$  is chosen by saturating the inequality so that the HDE density is

$$\rho_{\text{de}} = 3c^2 M_{\text{pl}}^2 L^{-2} , \quad (1)$$

where  $c$  is a numerical constant, and  $M_{\text{pl}} \equiv 1/\sqrt{8\pi G}$  is the reduced Planck mass. If we take  $L$  as the size of the current Universe, for instance the Hubble scale  $H^{-1}$ , then the dark energy density estimated with Eq.(1) will be close to the observed value. However, Hsu [6] pointed out that this yields a wrong equation of state for dark energy. Li [7] subsequently proposed that the future event horizon to be chosen as the IR cut-off  $L$ , viable HDE models can then be constructed. As demonstrated in Ref. [7], the HDE scenario may help to answer the *fine tuning problem* and the *coincidence problem* of dark energy.

Various aspects of the HDE model and its extensions have been investigated subsequently. For example, it has been generalized to the case of non-flat Universe [10], it was studied from the perspective of the anthropic principle [11]. The holographic dark energy was also considered for driving the inflation, and its resulting power spectrum index calculated [12]. Ref. [13] defined a new future event horizon as the infrared cut-off  $L$ , and find that the coincidence problem could be alleviated to some extent. Ref. [14] investigated the possible form of the cut off scale  $L$  for the solution of coincidence problem. Inspired by the HDE model, Ref. [15] proposed the Ricci scalar curvature radius as  $L$ . The model was reconstructed with a scalar field [16]. Observational constraint have also been studied [17, 18].

Interaction between the DE and DM components were considered for the HDE model [19, 20]. Ref.[19] suggested that for the  $L = H^{-1}$  case, with interactions between the two dark components, the dark energy could acquired an equation of state in agreement with observations, thus partly solved the no-acceleration problem noted in Ref.[7] for interaction-free models. Ref.[20] generalized the discussion in Ref.[19] to the case of future event horizon. In that paper the proposed form of interaction is  $3H\rho_{tot}$ , which could also leads to a negative dark energy equation of state.

However, Ref.[21] pointed out that the interaction terms such as  $Q \sim 3H\rho_{tot}$ ,  $3H\rho_{de}$ ,  $3H\rho_m$  all lead to unphysical results, because the dark matter density could be driven to negative value in these models.

Here we propose a form of interaction which we considered *natural* and *physically plausible*. In general, when two types of matter interact with each other, the interaction should be proportional to the product of the powers of the number density of both. This is most easily understood in the following way: if one component does not exist, then there certainly would have no interaction at all, with its amount increasing, the interaction rate should increase. Thus, at least in the diffuse limit, the interaction rate should be proportional to some powers of the density (the relation could become more complicated when the densities become high). For instance, this is the case for ordinary two-body chemical reactions, namely

$$a^{-3} \frac{d(n_1 a^3)}{dt} \sim n_1 n_2 \langle \sigma v \rangle, \quad (2)$$

i.e. the reaction rate is proportional to the product of number densities of the two particle species.

However, besides the interaction in the usual sense (“scattering”), one may also consider a more general case where the dark energy is converted to dark matter or vice versa by “annihilation” or “decay”. In such a case, the “interaction term” or more precisely the energy exchange term would depend only on one of the densities and not on the other.

In general, we consider the interaction term to be proportional to some powers of the density,

$$\dot{\rho}_m + 3H\rho_m = \gamma\rho_m^\alpha\rho_\Lambda^\beta, \quad (3)$$

$$\dot{\rho}_\Lambda + 3H(1 + w_\Lambda)\rho_\Lambda = -\gamma\rho_m^\alpha\rho_\Lambda^\beta, \quad (4)$$

in which  $\rho_m$  and  $\rho_\Lambda$  are the energy densities of the matter and HDE respectively, and  $\gamma$  is a parameter with mass dimension  $[\text{density}^{\alpha+\beta-1} \times \text{time}]^{-1}$ . The power index  $\alpha, \beta$  is assumed

to satisfy

$$\alpha, \beta \geq 0.$$

where if one of them is 0, we will have the case of “decay” (if the other is 1) or “annihilation” (if the other is 2). If  $\gamma > 0$ , the interaction suggests that dark energy is converted into dark matter, while  $\gamma < 0$  suggests the inverse process. This form of interaction was considered in the study of coupled quintessence model [22]. However, not much research on this form of interaction was carried out to understand how such a coupling term would affect the evolution of the Universe.

In the next section, we present the evolution equations for the interacting holographic dark energy model (details of our derivation is given in the Appendix). In Sec. 3, we study the dynamical behavior of the model. In Sec.4 we explore the parameter space and find the best-fit and allowed region of  $\alpha, \beta$ . Finally, concluding remarks are given in Sec. 5.

## II. THE MODEL

Now let us consider a spatially flat Friedmann-Robertson-Walker (FRW) Universe filled with matter component  $\rho_m$ , HDE component  $\rho_\Lambda$  and the radiation  $\rho_r$ . For simplicity we do not distinguish dark matter and ordinary matter below but incorporate both in the matter component  $\rho_m$ . It is certainly possible or even likely that dark energy only couples to dark matter. However, in that case the baryons simply evolves as  $\rho_b \sim a^{-3}$  where  $a$  is the scale factor, the baryon component would then become dynamically irrelevant as the Universe expands, so it only affects the details of the model but not its qualitative behavior, hence we will neglect this effect in the present paper. The Friedmann equation reads

$$3M_{pl}^2 H^2 = \rho_m + \rho_\Lambda + \rho_r, \quad (5)$$

where  $\rho_r$  is the energy density of the radiation which satisfies  $\rho_r \sim a^{-4}$ . Thus, Eqs. (1), (3), (4), (5) are the dynamic equations which uniquely determine the evolution of  $\rho_m(z)$ ,  $\rho_\Lambda(z)$ ,  $\rho_r(z)$ ,  $w_\Lambda(z)$  and  $H(z)$ . In Eq.(1),  $L$  could be Hubble horizon  $H^{-1}$ , particle horizon and future event horizon, i.e.

$$L = R_{ph}(t) = a(t) \int_0^a \frac{da'}{H' a'^2}, \quad (6)$$

or

$$L = R_{eh}(t) = a(t) \int_a^\infty \frac{da'}{H' a'^2}. \quad (7)$$

We define the following dimensionless quantities:  $\tilde{\rho}_m = \rho_m/\rho_{0cr}$ ,  $\tilde{\rho}_r = \rho_r/\rho_{0cr}$ ,  $\tilde{\rho}_\Lambda = \rho_\Lambda/\rho_{0cr}$ , where  $\rho_{0cr} = 3H_0^2 M_{pl}^2$  is the current critical density, and  $E(z) = H(z)/H_0$ , and introduce

$$\lambda = 3^{\alpha+\beta-1} \gamma H_0^{2(\alpha+\beta)-3} M_{pl}^{2(\alpha+\beta)-2} = \gamma \rho_{0cr}^{\alpha+\beta-1} H_0^{-1}, \quad (8)$$

The dimensionless  $\lambda$  parameter determines the characteristic strength of the interaction.

The equation of motion of HDE model for the particle (event) horizon cases are

$$\begin{aligned} \frac{d\tilde{\rho}_\Lambda}{dz} &= 2 \frac{\tilde{\rho}_\Lambda}{(1+z)} \left[ 1 \pm \frac{\tilde{\rho}_\Lambda^{\frac{1}{2}}}{c \cdot E(z)} \right], \\ \frac{dE(z)}{dz} &= \frac{1}{2(1+z)} \left[ 3E(z) + \frac{(\tilde{\rho}_r - \tilde{\rho}_\Lambda)}{E(z)} \pm \frac{2\tilde{\rho}_\Lambda^{\frac{3}{2}}}{c \cdot E^2(z)} - \frac{\lambda(E(z)^2 - \tilde{\rho}_r - \tilde{\rho}_\Lambda)^\alpha \tilde{\rho}_\Lambda^\beta}{E(z)^2} \right], \\ w_\Lambda(z) &= -\frac{1}{3} \pm \frac{2}{3} \frac{\tilde{\rho}_\Lambda^{\frac{1}{2}}}{c \cdot E(x)} - \frac{\lambda}{3} \frac{1}{E(x)} [E(x)^2 - \tilde{\rho}_\Lambda - \tilde{\rho}_r]^\alpha \tilde{\rho}_\Lambda^{\beta-1}, \end{aligned} \quad (9)$$

in which the upper(lower) sign represents the case of particle(future event) horizon (c.f. Appendix for details of derivation). It is easy to verify that if  $L$  in Eq.(1) equals to particle horizon  $R_{ph}$  or Hubble horizon  $H^{-1}$ , the model cannot fit the current observational data, because current data prefer the dark energy with equation of state near  $-1$ , while in the above two cases the equation of state  $w$  will be always greater than  $-\frac{1}{3}$  (see also analysis in Ref.[7]). Therefore, in the following we will focus on the interacting model with  $L = R_{eh}$  (see Eq.(9)).

### III. DYNAMICAL BEHAVIORS

In this section we study the dynamical behavior in models with interaction between DE and DM, which may give raise to some interesting behaviors. First we consider the case where  $\alpha, \beta$  are fixed to be 1, then consider the more general cases.

As a typical example we consider the model with  $c = 0.81, \lambda = -0.03$ , which happens to be the  $\alpha = \beta = 1$  model which best fits the current data ( for details of the fitting procedure see next section). First we plot the evolution of densities of different components in Fig.1. While one might think that the coupling between DE and DM might help resolve the coincidence problem, we find that for these particular parameter values the evolution of different densities are rather similar to that of the standard  $\Lambda$ CDM model, i.e. the DM

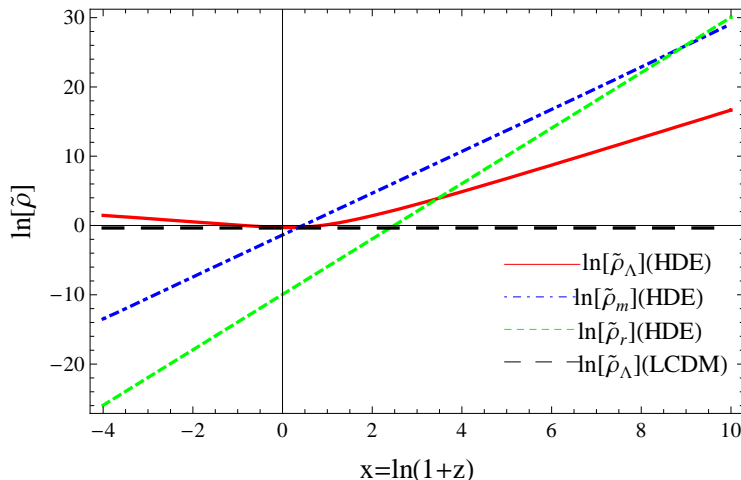


FIG. 1: Evolution of densities in the HDE model. The black-dashed line is the constant magnitude of dark energy in the LCDM universe. The evolutions of matter and radiation in LCDM model are very close to those (green-dashed and blue-dotted-dashed lines) in the HDE model.

and DE densities could still differ by orders of magnitude, so it does not seem to help much in this case. Rather, the fine tuning problem is solved as in other holographic dark energy models: the density of the dark energy is associated with the scale of horizon rather than the Planck scale, due to the holographic principle. We have also investigated cases with larger coupling constant  $\lambda$ . We find that indeed, for the strong coupling case ( $\lambda > 1$ ), the dark matter and dark energy could be made to evolve with comparable density for an extended range of redshifts, thus in some sense solving the “coincidence problem”. This is perhaps also true for any strongly coupled dark matter-dark energy model. However, for strong coupling the fit to observation is not good.

To investigate how the dynamics of the components are affected by coupling with the other component, one may compare the expansion term  $3H\rho_i$  ( $i = m, \Lambda$ ) with the interaction term  $\gamma\rho_m\rho_\Lambda$ . If the interaction term is greater than or comparable with the expansion term of both of the components, the two components are strongly coupled and evolves together. As the Universe expands, typically the density of the component would drops as  $a^{-3(1+w)}$ , the interaction term often drops much more rapidly than the expansion term. When the expansion term of a component is much greater than the interaction term, that component

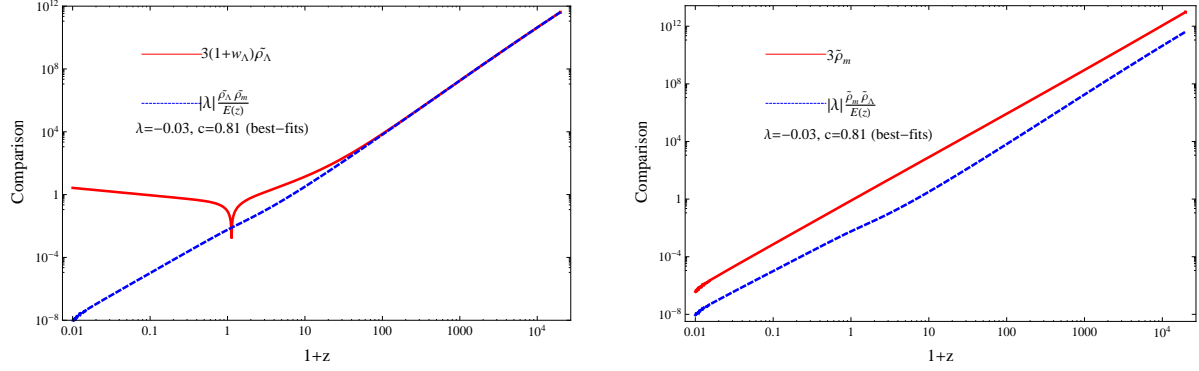


FIG. 2: Comparisons of the expansion term (red solid line) for dark energy (left panel) and dark matter (right) with the interaction term (blue dashed line) for the model with  $c = 0.81$ ,  $\lambda = -0.03$ .

evolves almost freely, and we may say the two components are decoupled<sup>1</sup>. The coupling and de-coupling effects between the two components could be asymmetric, as each has its own expansion term. It is possible that for one component the expansion term is greater, so it is decoupled from the other component, but for the other component, its expansion term is still smaller than or comparable with the interaction, thus it is still coupled to the other component.

In Fig. 2, we compare the expansion term of the dark energy and the dark matter with the interaction term as a function of redshift. In the left panel, we plot the magnitude of the dark energy expansion term  $3(1+w)\tilde{\rho}_\Lambda$ , and in the right panel, we plot the magnitude of the dark matter expansion term  $3\tilde{\rho}_m$ , as red solid lines. The interaction term  $|\lambda|\frac{\tilde{\rho}_m\tilde{\rho}_\Lambda}{E(z)}$  are plotted in both panels for comparison with the expansion terms. In the early Universe, the dark matter takes a greater proportion of the total density, and for dark energy the interaction term is comparable with the expansion term, so the dark energy is moderately coupled to the dark matter. Later, as the density of dark matter is diluted by expansion, the interaction term becomes negligible compared with the expansion term, and the dark

<sup>1</sup> Note here that in the literatures the word “decoupling” may refer to a number of different phenomena. For the decoupling of WIMP dark matter from the radiation-baryon fluid, what is discussed above (the evolution of density) is usually called “thermal decoupling”. There is also “kinetic decoupling” which refers to decoupling of temperature (see, e.g., [23]). Admittedly, this nomenclature is somewhat confusing, since one might naively think that “thermal decoupling” refers to decoupling of temperature, and “kinetic decoupling” refers to decoupling of density evolution! Below we shall refer the decouplings discussed here as “dynamical decoupling”, the term “thermal decoupling” and “kinetic decoupling” is not used in this paper.

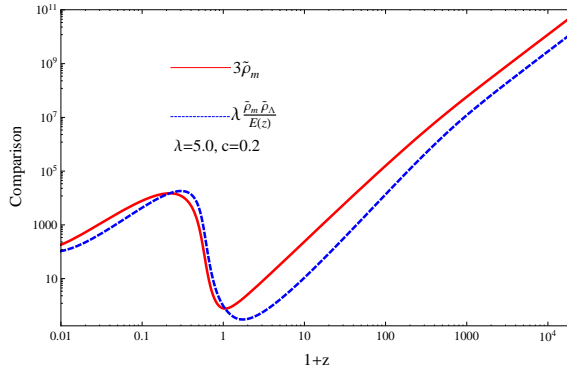


FIG. 3: Comparisons of the expansion term (red solid line) for dark matter with the interaction term (blue dashed line) for the model with  $c = 0.2$ ,  $\lambda = 5$ .

energy is decoupled from dark matter. In the right panel of Fig. 2, we plot the dark matter expansion term  $3\tilde{\rho}_m$  and interaction term  $\lambda \frac{\tilde{\rho}_m \tilde{\rho}_\Lambda}{E(z)}$  as a function of redshift  $z$ . We see that throughout the cosmic history, for the dark matter the expansion term is always greater than the interaction term, so the dark matter is at most weakly coupled to dark energy. Such decoupling history is quite typical for many interactions.

However, there could also be some quite unexpected and interesting behavior in the presence of dark energy. In Fig. 3, we plot the dark matter expansion term and the interaction for the model with  $c = 0.2$ ,  $\lambda = 5$ , which is chosen to illustrate such unusual behavior. In this model, because  $w < -1$ , the dark energy density actually increases at later time. Interestingly, we see that initially the interaction term of the dark matter is smaller than the expansion term, so the dark matter is only weakly coupled to dark energy, but at later time, the interaction term becomes comparable with the expansion term of dark matter, so the DM becomes coupled to DE. This is the reverse of the familiar decoupling process, which we shall call *incoupling*. This strange and interesting behavior could only occur when a component is coupled to dark energy, whose density does not decrease during the cosmic expansion. As the DE keeps being converted into DM, the DM evolution is greatly affected by DE. This model does not yield good fit to the observational data, but is only used for illustrate an interesting dynamical behavior in the presence of  $w < -1$  dark energy.

In Fig.4, we plot the evolution of  $H$  for three choices of  $c$  parameter, i.e. the best fit  $c_0 = 0.81$ , and  $c_0 \pm \sigma_c$ , while keeping  $\lambda = -0.03$ . The Hubble parameter for the  $\Lambda$ CDM model is also plotted for comparison. We also plot the equation of state of the dark energy



for these models in Fig. 5. On the left panel, curves for different  $c$  but identical  $\lambda$  are plotted; on the right panel, curves for identical  $c$  but different  $\lambda$  are plotted. In all of these model, the phantom divide  $w = -1$  is either crossed, or will be crossed in the near future. The dark energy density would keep increasing, the interaction with DM would not slow it down, as the dark energy has become decoupled to the DM. Eventually a “Big Rip” would occur. The current value of the equation of state  $w_0$  for the best fit model  $c = 0.81, \lambda = -0.03$  is around  $-1.04$ , which is within the  $1\sigma$  CL region of  $w_0$  in the WMAP 5 years results[24], suggesting that this model is consistent with the current observations.

The value of  $\lambda$  in these models does not significantly affect the fate of the Universe, but it does greatly affect the past evolution. This result is easy to understand, as the dark energy dynamically decouples from dark matter, the interaction become negligible, regardless the precise value of coupling constant. The eventual fate of the Universe in this interacting holographic dark energy model is qualitatively similar to those without interactions, though the details of the evolution would be different. Thus, as in the case of non-interacting holographic models, for the fate of the Universe,  $c < 1$  leads to phantom-like behavior and Big Rip[25], while  $c > 1$  leads to quintessence behavior. This is very different from the models discussed in Ref. [17].

We now consider the more general case of  $\alpha, \beta \neq 1$ . We plot the equation of state in Fig. 6, varying  $\alpha$  in the left panel while keeping  $\beta = 1$ , and varying  $\beta$  in the right panel while

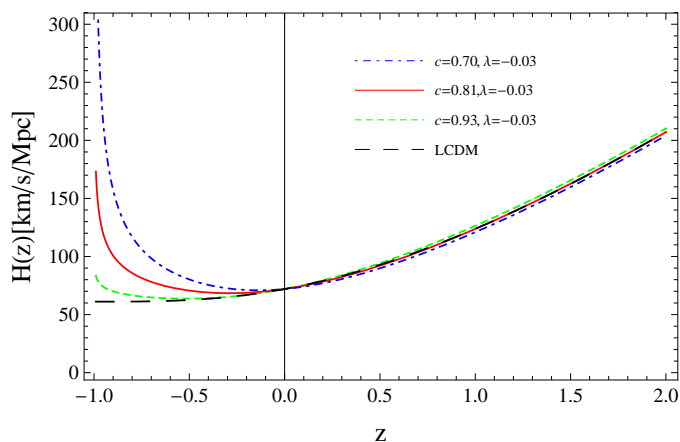


FIG. 4: Evolution of Hubble rate for three choices of parameter  $c$ , three curves (red, blue, and green one) are the best fit, and  $\pm 1\sigma_c$  C.L. values. Here we set  $\Omega_{m0} = 0.26, H_0 = 72\text{km/s/Mpc}$ . The black-dashed line is the Hubble parameter in the LCDM universe.

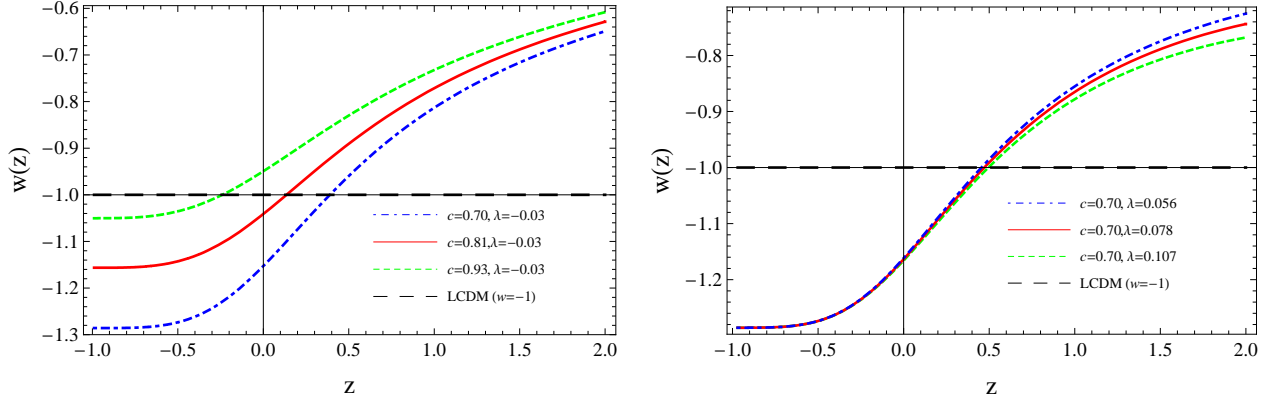


FIG. 5: Equation of state with  $\alpha = \beta = 1$  for several parameters. The black-dashed line is the constant equation of state in the LCDM universe.

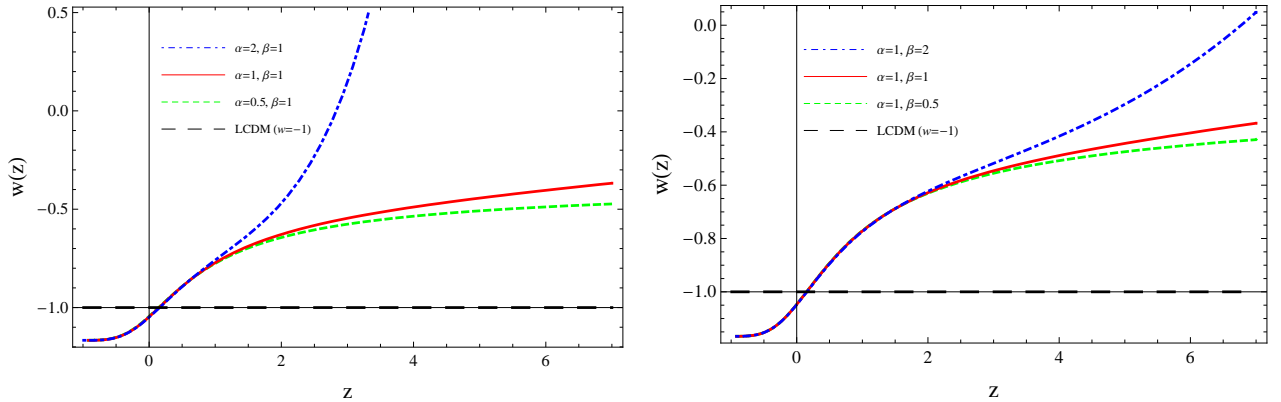


FIG. 6: Redshift evolution of the equation of state, with the best fit values of  $c$ ,  $\lambda$  and  $\Omega_{m0}$ . The black-dashed line is the constant equation of state in the LCDM universe.

keeping  $\alpha = 1$ . The other parameters are kept as before. For  $\alpha < 1$ , the equation of state for dark energy is slightly more negative. For  $\alpha > 1$ , at higher redshift  $\rho_m^\alpha$  increases rapidly, and the coupling term would become very large, the whole system would be dominated by the evolution of matter. However, such a model would not really fit the low redshift observation, so it would not be relevant to our purpose. For large  $\beta$ , we can also see that the equation of state of dark energy  $w > -1$  at high  $z$ , but the variation is not as rapid as in the case of  $\alpha$ , this is because the dark energy component does not increase as much as the dark matter component. Still, this makes poor fit to the observational data.

Anyway, for the case  $\alpha, \beta \gg 1$ , Eq.(A16) is reduced to

$$w_\Lambda(x) \simeq -\frac{\lambda \tilde{\rho}_\Lambda^{\beta-1}}{3 E(x)} (E(x)^2 - \tilde{\rho}_\Lambda - \tilde{\rho}_r)^\alpha. \quad (10)$$

Substituting this equation into Eq.(A4) and making use of Eq.(A1), we obtain the following approximate equation for  $\tilde{\rho}_\Lambda$

$$\tilde{\rho}'_\Lambda \simeq 3\tilde{\rho}_\Lambda, \quad (11)$$

for which the solution will simply be

$$\tilde{\rho}_\Lambda(a) \simeq B/a^3, \quad (12)$$

where  $B$  is a constant. This scaling behavior of dark energy density (if  $\alpha, \beta \gg 1$ ) is very similar to that of the Chaplygin gas model [26], which at the high redshift also has the scaling behavior as  $a^{-3}$  while at the low redshift has the constant magnitude. However, in the present case it does not provide a good fit to the observations.

#### IV. FITTING THE MODEL

Now we fit the model parameters with the current observational data. We use three kinds of observations, the first one is type Ia supernovae (SNIa) which serves as the standard candle; the second is the baryon acoustic oscillation (BAO) in large scale structure of galaxy distribution, the third is the the cosmic microwave background anisotropies, the latter two provides standard ruler at different redshifts. For the flat geometry we are considering,  $d_L = (1+z)^2 d_A = (1+z)r$ , where  $d_L, d_A, r$  are the luminosity distance, angular diameter distance and comoving coordinate distance, respectively, and  $r$  is given by  $r = \frac{c}{H_0} \int_0^z \frac{dz'}{E(z')}$ , which could be calculated for each model by solving Eq. (9) or Eqs. (A17)-(A18).

For the SNe Ia, we use the data set published by Supernova Cosmology Project (SCP) team recently [27]. This data set contains 307 selected SNe Ia which includes several current widely used SNe Ia data set, such as those collected by the Hubble Space Telescope (HST) [28, 29], the SuperNova Legacy Survey (SNLS) [30] and the Equation of State: SuperNovae trace Cosmic Expansion (ESSENCE) surveys[31]. Using the same analysis procedure and improved selection approach, all of the sub data sets are analyzed to obtain a consistent and high-quality ‘‘Union’ SNe Ia data set, which provides tighter and more reliable constraints for our models. For the BAO data, we use the data given in Percival *et al.* [32] and WMAP

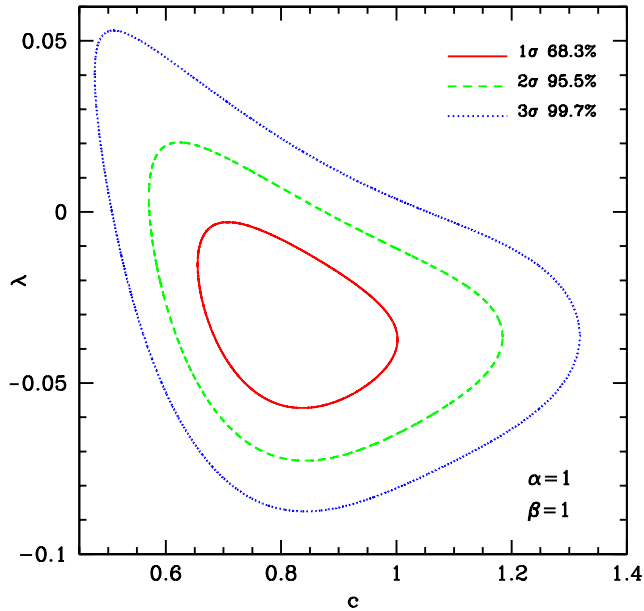


FIG. 7: Contours of  $\lambda$  versus  $c$  for  $\alpha = \beta = 1$ .

team [24]. We use the quantity  $r_s/D_v$  which is determined by the Sloan Digital Sky Survey (SDSS) ( $z = 0.35$ ) and the Two Degree Field Galaxy Redshift Survey (2dFGRS) ( $z = 0.2$ ) in our constraints, where  $r_s$  is the co-moving sound horizon size at the decoupling epoch, and  $D_v$  is the effective distance defined by Eisenstein *et al.* [33]. Since this quantity is just a ratio of two “standard ruler”, it could give a reliable measurement of the expansion history of the Universe. For the CMB, we use the position of the first peak of the Cosmic Microwave Background (CMB) angular power spectrum  $\ell_1$ . The details of this technique was described in our earlier paper Ref. [34].

We use the Markov Chain Monte Carlo (MCMC) method to constrain the parameters with the combined data set of SN Ia+BAO+CMB (for details of our implementation of this technique, see Ref. [35]). In the present model, the relevant parameters are the matter density  $\Omega_{m0}$ , Hubble constant  $H_0$ , and the holographic dark energy parameter  $c, \lambda$ . We marginalize over  $H_0$  and  $\Omega_{m0}$ . For  $\alpha, \beta$ , we limit their range to  $0 < \alpha, \beta < 2$ . As discussed in the last section, greater values of  $\alpha, \beta$  would not yield good fit to observation.

For the fixed  $\alpha = \beta = 1$  case, as can be seen in Fig. 7, the best fit value and error on  $c, \lambda$  are

$$c = 0.81^{+0.12}_{-0.11}, \quad \lambda = -0.03 \pm 0.02. \quad (13)$$

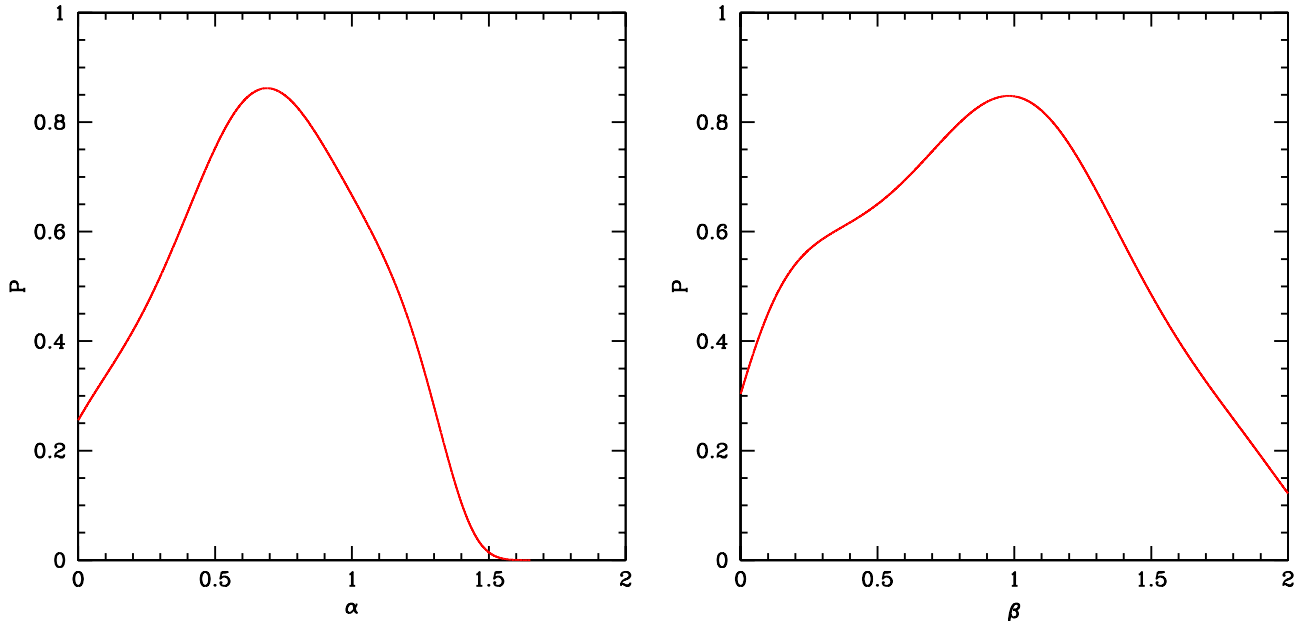


FIG. 8: Probability distribution function of the power index parameters  $\alpha$  and  $\beta$ .

The behavior of the best fit model has been discussed as the example given in the previous section. The models within the  $1\sigma$  contour also exhibit similar behavior.

Now we let  $\alpha, \beta$  be free parameters, the PDF of  $\alpha$  and  $\beta$  are shown in Fig. 8. The best fit value for  $\alpha, \beta$  are  $\alpha = 0.69_{-0.38}^{+0.45}$  and  $\beta = 0.98_{-0.81}^{+0.49}$ . If one demand  $\alpha, \beta$  to be integers for physical reasons, then  $\alpha = 1, \beta = 1$  is still the best fit. Alternatively, non-integer power may rise if the interaction is complicated. The best fit for  $c$  and  $\lambda$  are  $c = 0.81_{-0.11}^{+0.13}$  and  $\lambda = -0.04_{-0.04}^{+0.03}$ , as shown in Fig. 9, it is not too different from the  $\alpha = \beta = 1$  case.

## V. CONCLUSION

In the framework of holographic dark energy model, we proposed a form of interaction between dark energy and dark matter which we considered to be natural and physically plausible. That is, the interaction rate is proportional to the product of powers of the dark energy and dark matter densities  $\rho_m^\alpha \rho_\Lambda^\beta$ . For this type of interaction, we find that for the weak coupling case (the dimensionless coupling constant  $\lambda < 1$ , see Eq. (8)), the ultimate fate of the Universe is similar to the case of non-interacting holographic dark energy, namely for  $c < 1$  the equation of state of the dark energy will cross  $w = -1$ , and behave like a phantom in the future, and the Universe ends in a Big Rip. We also discovered the interesting

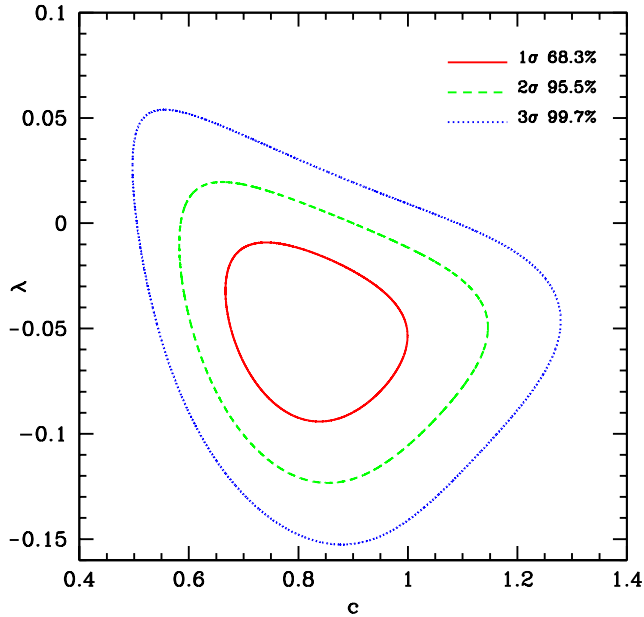


FIG. 9: Contours of  $\lambda$  versus  $c$  for free  $\alpha$  and  $\beta$ .

phenomenon of *incoupling*, which occurs only when the dark matter is coupled to dark energy. This is the opposite of the familiar process of *decoupling*, the dark matter become increasingly coupled to the dark energy as Universe expands. We then use the currently available observational data to constrain the parameters of this model. The data set we used include 307 selected SNIa published by the SCP team [27], baryon acoustic oscillation from SDSS and 2dFGRS [32], as well as the position of the first peak of the CMB angular power spectrum [24]. We find that the best fit form of interaction is  $\alpha = 0.69, \beta = 0.98$ . If one requires  $\alpha, \beta$  to be integers for reasons of fundamental physics, then the most favored interaction rate is proportional to the product of the density of dark matter and dark energy.

### Acknowledgments

Our MCMC chain computation was performed on the Supercomputing Center of the Chinese Academy of Sciences and the Shanghai Supercomputing Center. This work is supported by the Chinese Academy of Sciences under grant KJCX3-SYW-N2, by the Ministry of Science and Technology National Basic Science program (project 973) under grant No.2007CB815401, and by the National Science Foundation of China under the Distinguished Young Scholar Grant 10525314, and the Key project Grants No.10503010.

## APPENDIX A: DYNAMICAL EQUATIONS

We give the detailed derivation of the dynamical equations of the interacting holographic dark energy model here. Using the dimensionless notations given in Sec.2, we have

$$E(x)^2 = \tilde{\rho}_m + \tilde{\rho}_\Lambda + \tilde{\rho}_r, \quad (\text{A1})$$

$$\tilde{\rho}_r = \Omega_{r0} e^{4x}, \quad (\text{A2})$$

$$\tilde{\rho}'_m - 3\tilde{\rho}_m = -\lambda \frac{\tilde{\rho}_m^\alpha \tilde{\rho}_\Lambda^\beta}{E(x)}, \quad (\text{A3})$$

$$\tilde{\rho}'_\Lambda - 3(1 + w_\Lambda)\tilde{\rho}_\Lambda = \lambda \frac{\tilde{\rho}_m^\alpha \tilde{\rho}_\Lambda^\beta}{E(x)}, \quad (\text{A4})$$

$$\tilde{\rho}_\Lambda = \frac{c^2}{H_0^2 L^2} = \frac{c^2}{H^2 L^2} E(x)^2. \quad (\text{A5})$$

so

$$\tilde{\rho}'_\Lambda = \frac{d}{dx} \tilde{\rho}_\Lambda = \left(-2 \frac{L'}{L}\right) \tilde{\rho}_\Lambda, \quad (\text{A6})$$

$$E(x) \cdot E(x)' = \frac{3}{2} [\tilde{\rho}_m + (1 + w_\Lambda)\tilde{\rho}_\Lambda + \frac{4}{3}\tilde{\rho}_r]. \quad (\text{A7})$$

By substitute Eq.(A6) into Eq. (A4), we have

$$w_\Lambda(x) = -1 - \frac{2 L'(x)}{3 L(x)} - \frac{\lambda \tilde{\rho}_m(x)}{3 E(x)}. \quad (\text{A8})$$

If  $L$  is taken to be the particle horizon (Eq.(6)) or future event horizon (Eq.(7)), the derivative of  $L$  is

$$L' = -(L \pm \frac{1}{H}), \quad (\text{A9})$$

where the upper (lower) sign represents particle horizon (future event horizon). By substituting Eq. (A9) and (A5) into Eq. (A8), we have the equation of state in the particle horizon (upper sign) and future event horizon (lower sign) cases

$$w_\Lambda(x) = -\frac{1}{3} \pm \frac{2}{3} \frac{\tilde{\rho}_\Lambda^{\frac{1}{2}}}{c \cdot E(x)} - \frac{\lambda \tilde{\rho}_m(x)^\alpha \tilde{\rho}_\Lambda(x)^{\beta-1}}{3 E(x)} \quad (\text{A10})$$

Substituting Eq. (A10) into (A7), we have

$$2E(x) \cdot E'(x) = 3(\tilde{\rho}_m + \frac{4}{3}\tilde{\rho}_r) + 2\tilde{\rho}_\Lambda \pm 2 \frac{\tilde{\rho}_\Lambda^{\frac{3}{2}}}{c \cdot E(x)} - \frac{\lambda}{E(x)} \tilde{\rho}_m^\alpha \tilde{\rho}_\Lambda^\beta. \quad (\text{A11})$$

Taking derivative of Eq. (A1) with respect to  $x$ , we have

$$2E(x) \cdot E'(x) = \tilde{\rho}'_m + \tilde{\rho}'_\Lambda + 4\tilde{\rho}_r, \quad (\text{A12})$$

Substituting Eq. (A3) into Eq. (A12), we obtain

$$2E(x) \cdot E'(x) = 3\tilde{\rho}_m + \tilde{\rho}'_\Lambda + 4\tilde{\rho}_r - \frac{\lambda}{E(x)} \tilde{\rho}_m^\alpha \tilde{\rho}_\Lambda^\beta. \quad (\text{A13})$$

Subtract equations (A13) from (A12), we obtain the following simple dynamical equation:

$$\tilde{\rho}'_\Lambda = 2\tilde{\rho}_\Lambda \left[ 1 \pm \frac{\tilde{\rho}_\Lambda^{\frac{1}{2}}}{c \cdot E(x)} \right], \quad (\text{A14})$$

Eliminate  $\tilde{\rho}_m$  in Eq. (A11) using Eq.(A1),

$$E'(x) = \frac{3}{2}E(x) + \frac{1}{2E(x)}(\tilde{\rho}_r - \tilde{\rho}_\Lambda) - \frac{\lambda}{2E(x)^2}(E(x)^2 - \tilde{\rho}_r - \tilde{\rho}_\Lambda)^\alpha \tilde{\rho}_\Lambda^\beta \pm \frac{\tilde{\rho}_\Lambda^{\frac{3}{2}}}{c \cdot E^2(x)}. \quad (\text{A15})$$

and

$$w_\Lambda(x) = -\frac{1}{3} \pm \frac{2}{3} \frac{\tilde{\rho}_\Lambda^{\frac{1}{2}}}{c \cdot E(x)} - \frac{\lambda}{3} \frac{\tilde{\rho}_\Lambda^{\beta-1}}{E(x)} (E(x)^2 - \tilde{\rho}_r - \tilde{\rho}_\Lambda)^\alpha, \quad (\text{A16})$$

To make Eq. (A14) and (A15) easy to solve numerically, we change the variable to  $z$ ,

$$\frac{d\tilde{\rho}_\Lambda}{dz} = 2 \frac{\tilde{\rho}_\Lambda}{(1+z)} \left[ 1 \pm \frac{\tilde{\rho}_\Lambda^{\frac{1}{2}}}{c \cdot E(z)} \right], \quad \tilde{\rho}_\Lambda(0) = 1 - \Omega_{m0}, \quad (\text{A17})$$

$$\begin{aligned} \frac{dE(z)}{dz} &= \frac{1}{(1+z)} \left[ \frac{3}{2}E(z) + \frac{1}{2E(z)}(\tilde{\rho}_r - \tilde{\rho}_\Lambda) \pm \frac{\tilde{\rho}_\Lambda^{\frac{3}{2}}}{c \cdot E^2(z)} \right. \\ &\quad \left. - \frac{\lambda}{2E(z)^2}(E(z)^2 - \tilde{\rho}_r - \tilde{\rho}_\Lambda)^\alpha \tilde{\rho}_\Lambda^\beta \right], \\ E(0) &= 1, \end{aligned} \quad (\text{A18})$$

where

$$\tilde{\rho}_r = \Omega_{r0}(1+z)^4 = 4.78 \times 10^{-5}(1+z)^4, \quad (\text{A19})$$

and the upper (lower) sign in Eq. (A17) and (A18) corresponds to the model with particle (future event) horizon. Thus, Eq. (A17) and (A18) are the complete system of equations. In the limit  $\lambda = 0$  and  $\rho_r = 0$ , the equations reduce to non-interacting holographic dark energy model [7, 36].

- 
- [1] A. G. Riess *et al.* [Supernova Search Team Collaboration], *Astron. J.* **116**, 1009 (1998) [astro-ph/9805201]; S. Perlmutter *et al.* [Supernova Cosmology Project Collaboration], *Astrophys. J.* **517**, 565 (1999) [astro-ph/9812133].



- [2] D. N. Spergel *et al.* [WMAP Collaboration], *Astrophys. J. Suppl.* **148**, 175 (2003) [astro-ph/0302209]; D. N. Spergel *et al.*, *Astrophys. J. Suppl.* **170**, 377 (2007) [astro-ph/0603449].
- [3] M. Tegmark *et al.* [SDSS Collaboration], *Phys. Rev. D* **69**, 103501 (2004) [astro-ph/0310723]; K. Abazajian *et al.* [SDSS Collaboration], *Astron. J.* **128**, 502 (2004) [astro-ph/0403325]; K. Abazajian *et al.* [SDSS Collaboration], *Astron. J.* **129**, 1755 (2005) [astro-ph/0410239].
- [4] A. G. Cohen, D. B. Kaplan and A. E. Nelson, *Phys. Rev. Lett.* **82**, 4971 (1999) [hep-th/9803132].
- [5] P. Horava and D. Minic, *Phys. Rev. Lett.* **85**, 1610 (2000) [hep-th/0001145]; S. D. Thomas, *Phys. Rev. Lett.* **89**, 081301 (2002).
- [6] S. D. H. Hsu, *Phys. Lett. B* **594**, 13 (2004) [hep-th/0403052].
- [7] M. Li, *Phys. Lett. B* **603**, 1 (2004) [hep-th/0403127].
- [8] G. 't Hooft, gr-qc/9310026; L. Susskind, *J. Math. Phys.* **36**, 6377 (1995) [hep-th/9409089].
- [9] J. D. Bekenstein, *Phys. Rev. D* **7**, 2333 (1973); J. D. Bekenstein, *Phys. Rev. D* **9**, 3292 (1974); J. D. Bekenstein, *Phys. Rev. D* **23**, 287 (1981); J. D. Bekenstein, *Phys. Rev. D* **49**, 1912 (1994); S. W. Hawking, *Commun. Math. Phys.* **43**, 199 (1975); S. W. Hawking, *Phys. Rev. D* **13**, 191 (1976).
- [10] Q. G. Huang and M. Li, *JCAP* **0408**, 013 (2004) [astro-ph/0404229].
- [11] Q. G. Huang and M. Li, *JCAP* **0503**, 001 (2005) [hep-th/0410095]
- [12] K. Enqvist and M. S. Sloth, *Phys. Rev. Lett.* **93**, 221302 (2004) [hep-th/0406019]; B. Chen, M. Li and Y. Wang, *Nucl. Phys. B* **774**, 256 (2007) [arXiv:astro-ph/0611623].
- [13] S. Nojiri and S. D. Odintsov, *Gen. Rel. Grav.* **38**, 1285 (2006) [hep-th/0506212];
- [14] B. Hu and Y. Ling, *Phys. Rev. D* **73**, 123510 (2006) [hep-th/0601093].
- [15] C. J. Gao, X. L. Chen, Y. G. Shen, arXiv:0712.1394 [astro-ph].
- [16] X. Zhang, *Phys. Lett. B* **648**, 1 (2007) [astro-ph/0604484]; Y. Z. Ma and X. Zhang, *Phys. Lett. B* **661**, 239 (2008) 0709.1517 [astro-ph].
- [17] Y. Z. Ma, Y. Gong and X. Chen, *Eur. Phys. J. C* **60** (2009) 303, 0711.1641 [astro-ph].
- [18] X. Zhang, *Int. J. Mod. Phys. D* **14**, 1597 (2005) [astro-ph/0504586].
- [19] D. Pavon and W. Zimdahl, *Phys. Lett. B* **628**, 206 (2005) [gr-qc/0505020].
- [20] B. Wang, Y. Gong and E. Abdalla, *Phys. Lett. B* **624**, 141 (2005) [hep-th/0506069]; C. Feng, B. Wang, Y. Gong and R. K. Su, 0706.4033 [astro-ph].

- [21] M. Li, C. Lin and Y. Wang, JCAP **05**, 023 (2008), 0801.1407 [astro-ph].
- [22] G. Mangano, G. Miele and V. Pettorino, Mod. Phys. Lett. A **18**, 831 (2003), [astro-ph/0212518].
- [23] X. Chen, M. Kamionkowski, and X. Zhang, Phys. Rev. **D** 64, 021302 (2001), [astro-ph/0103452].
- [24] E. Komastu *et al.*, 0803.0547 [astro-ph].
- [25] R.R. Caldwell, Phys. Lett. B **45**, 23 (2002), [astro-ph/9908168].
- [26] N. Bilic, G. B. Tupper, R. D. Viollier, astro-ph/0207423; N. Bilic, G. B. Tupper, R. D. Viollier, Phys. Lett. B **535** (2002) 17-21, [astro-ph/0111325]; M. C. Bento, O. Bertolami, A. A. Sen, Phys. Rev. D **66** (2002) 043507, [gr-qc/0202064].
- [27] M. Kowalski *et al.*, arXiv: 0804.4142 [astro-ph].
- [28] A. G. Riess *et al.*, Astrophys. J. **607**, 665-687, (2004), [astro-ph/0402512].
- [29] A. G. Riess *et al.*, Astrophys. J. **659**, 98-121, (2007), [astro-ph/0611572].
- [30] P. Astier *et al.*, Astron. Astrophys. **447**, 31-48 (2006), [astro-ph/0510447].
- [31] W. M. Wood-Vasey *et al.*, arXiv: astro-ph/0701041.
- [32] W. J. Percival *et al.*, MNRAS **381**, 1053, (2007), arXiv:0705.3323 [astro-ph].
- [33] D. J. Eisenstein *et al.*, Astrophys. J. **633**, 560-574 (2005), [astro-ph/0501171].
- [34] Y. Gong and X. Chen, Phys. Rev. D **77**, 103511 (2008), arXiv:0802.2296 [astro-ph].
- [35] Y. Gong and X. Chen, Phys. Rev. D **76**, 123007 (2007), arXiv:0708.2977 [astro-ph].
- [36] Q. Wu, Y. Gong, A. Zhong and J. S. Alcaniz, arXiv:0705.1006 [astro-ph].